J. Fac. Sci. Univ. Tokyo
Sect. IA, Math.
33 (1986), 523-539.

An application of the charge simulation method to a free boundary problem

By Mayumi SHŌJI

Abstract. We consider a free boundary problem of a circulating flow around an equator of a celestial body. The flow is assumed to be a stationary, two-dimensional and irrotational one.

Previously, we investigated the bifurcating solutions from a trivial flow by the boundary element method regarding the same problem.[2] Then the numerical computation was successful only in simulating bifurcating solutions where the nonlinearity is of a limited extent.

Recently, better results are achieved in less CPU time by applying the charge simulation method. This method, however, is not yet analyzed mathematically, and leaves much room for improvement. In this paper, we report of and discuss these matters.

§ 1. Introduction.

We consider a stationary free boundary problem for an irrotational flow of a perfect fluid which is considered in [2].

Our purpose is a numerical simulation of bifurcating solutions of this problem by use of the charge simulation method. The problem is formulated as follows:

Problem. Find a closed Jordan curve γ outside the unit circle Γ in $\boldsymbol{R}^2$ and a stream function V such that the conditions (1.1)-(1.5) below are satisfied:

$$\Delta V=0 \quad \text{in} \quad \Omega_\gamma, \tag{1.1}$$

$$V=0 \quad \text{on} \quad \Gamma, \tag{1.2}$$

$$V=a \quad \text{on} \quad \gamma, \tag{1.3}$$

$$\frac{1}{2}|\nabla V|^2-\frac{g}{r}+\sigma K_\gamma=\text{unknown constant} \quad \text{on} \quad \gamma, \tag{1.4}$$

$$|\Omega_\gamma|=\omega_0. \tag{1.5}$$

Here we have used the following notation:

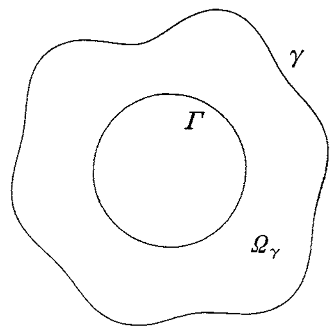

Figure 1

Ω_γ: the doubly connected domain between Γ and γ.
a, σ and ω_0: prescribed positive constants.
r: the distance from the origin.
K_γ: the curvature of γ, the sign of which is chosen to be positive in case that γ is convex.
$|\Omega_\gamma|$: the area of Ω_γ.

REMARK. The circle Γ represents the equator of the celestial body. The conditions (1.2) and (1.3) imply that each of Γ and γ is a streamline. The condition (1.4) is from Bernoulli's law in the presence of surface tension. The constant σ represents the coefficient of surface tension. The parameter a is important in that it measures the magnitude of the flow speed. Indeed, since V is proportional to a, the speed is large when a is large.

In this problem, the following (1) and (2) have been obtained analytically (see [4, 5, 6, 7]).
(1) For each a, there is a solution which is rotationary invariant; i.e., if we put

γ_0=the circle of radius r_0 with the origin as its center (the radius r_0 is a positive root of $\pi(r_0^2-1)=\omega_0$),

$$V_0=V_0(r)=\frac{a}{\log r_0}\log r \qquad (1<r<r_0),$$

then $\gamma=\gamma_0$ and $V=V_0$ give a solution, and we call this a trivial solution. This is a solution which is invariant under a natural action of the orthogonal group $O(2)$.

(2) If $a=0$, there is no solution other than the trivial one. But for $a>0$, there is a solution different from the trivial solution. This nontrivial solution is no longer $O(2)$-invariant, but it has a symmetry corresponding to a certain subgroup of $O(2)$. Such nontrivial solutions bifurcate from the trivial solution, when the parameter a varies as a control parameter and passes one of bifurcation points $\{a_n\}$. These a_n $(n=1, 2, \cdots)$ are written explicitly as

$$a_n=\left(\frac{\sigma(n^2-1)+g}{(1+nR_n)r_0}\right)^{1/2} r_0 \log r_0, \quad \text{where } R_n=(r_0^n+r_0^{-n})/(r_0^n-r_0^{-n}).$$

The bifurcating solutions emanating from a_n are written in the polar coordinates as

$$\gamma=\{(r_0+\varepsilon\cos(n\theta)+O(\varepsilon^2), \theta);\ 0\leqq\theta<2\pi\},$$

where ε is a small positive number.

The nontrivial solutions are solutions which bifurcate from the trivial solution. To compute the above non-trivial bifurcating solutions, we have only to get zero-points of a certain mapping H which we describe below: First we reformulate the problem in terms of function spaces and abstract symbols.

$C^{3+\alpha}(S^1)$ $(0<\alpha<1)$: the Hölder space, and the usual norm of this space is denoted by $\|\ \ \|_{3+\alpha}$,

$X^{3+\alpha}=\{u\in C^{3+\alpha}(S^1);\ u(\theta)=u(-\theta)\}$,

γ_u: a closed Jordan curve which is represented in the polar coordinates as $(r_0+u(\theta), \theta)$ $(0\leqq\theta<2\pi)$ for a given $u\in X^{3+\alpha}$,

Ω_u: a doubly connected domain which is enclosed with γ_u and Γ,

V_u: the solution of the following Dirichlet problem:

$$\Delta V_u=0 \quad \text{in} \quad \Omega_u, \tag{1.1$'$}$$

$$V_u=0 \quad \text{on} \quad \Gamma, \tag{1.2$'$}$$

$$V_u=a \quad \text{on} \quad \gamma_u. \tag{1.3$'$}$$

Now we define a mapping $F=F(a;\cdot,\cdot)$ in the following way:

$$F(a;u,\xi)=(F_1(a;u,\xi), F_2(a;u,\xi)),$$

$$F_1(a;u,\xi)=\left(\frac{1}{2}|\nabla V_u|^2-\frac{g}{r}\right)\Big|_{\gamma_u}+\sigma K_u-\xi-\xi_0, \tag{1.4$'$}$$

$$(1.5)' \qquad F_2(a;\, u,\, \xi)=\frac{1}{2}\int_0^{2\pi}(r_0+u(\theta))^2 d\theta-\pi-\omega_0.$$

Here ξ is a real variable which represents the unknown constant in (1.4) and ξ_0 is a constant given by $\xi_0=(1/2)(a/r_0 \log r_0)^2-g/r_0+\sigma/r_0$. Next we define H as follows:

$$H=H(\varepsilon;\, \lambda,\, v,\, \xi)=(H_1,\, H_2,\, H_3): \boldsymbol{R}\times X^{3+\alpha}\times\boldsymbol{R}\longrightarrow X^{1+\alpha}\times\boldsymbol{R}\times\boldsymbol{R},$$

$$H_i(\varepsilon;\, \lambda,\, v,\, \xi)=\begin{cases}\dfrac{1}{\varepsilon}F_i(a_n+\lambda;\, \varepsilon\cos(n\theta)+\varepsilon v,\, \varepsilon\xi) & \text{for} \quad \varepsilon\neq 0,\\ D_u F_i(a_n+\lambda;\, 0,\, 0)(\cos(n\theta)+v(\theta))+D_\xi F_i(a_n+\lambda;\, 0,\, 0)\xi & \\ & \text{for} \quad \varepsilon=0,\end{cases}$$
$$(i=1,\, 2)$$

$$H_3(\varepsilon;\, \lambda,\, v,\, \xi)=\int_0^{2\pi} v(\theta)\cos(n\theta)d\theta,$$

where D_u or D_ξ means the Fréchet derivative with respect to u or ξ, respectively.
Then it is easy to see that

i) $H(\varepsilon;\, 0,\, 0,\, 0)=(0,\, 0,\, 0)$.
ii) For some small $\varepsilon>0$, $H(\varepsilon;\, \lambda,\, v,\, \xi)=(0,\, 0,\, 0)$ if and only if $\{a,\, \gamma_u,\, V_u\}$ is a bifurcating solution for $u(\theta)=\varepsilon\cos(n\theta)+\varepsilon v(\theta)$, $a=a_n+\lambda$.

We can show that H is a smooth mapping defined on some neighborhood of the origin in $\boldsymbol{R}\times X^{3+\alpha}\times\boldsymbol{R}$ into $X^{1+\alpha}\times\boldsymbol{R}\times\boldsymbol{R}$. Hence the existence of the zero point $(\lambda,\, v,\, \xi)$ of $H(\varepsilon;\, \cdot,\, \cdot,\, \cdot)=0$ for a given ε is ensured by the implicit function theorem.[2,4,5]

Now the fact ii) above is the basis for the following computations.

§2. Computation by the Charge Simulation Method.

In this section we will give our computational scheme. As described in §1, the solutions $\{a,\, \gamma_u,\, V_u\}$ bifurcating from a_n are such as $\gamma_u=\{(r_0+u(\theta),\, \theta)|\, u(\theta)=\varepsilon\cos(n\theta)+\varepsilon v(\theta),\, \cos(n\theta)\perp v(\theta),\, 0\leqq\theta<2\pi\}$. We will chase these bifurcating solutions one afer another along the a_n-branch, regarding ε as a control-parameter. Namely if ε is given, a bifurcating solution $\{a,\, \gamma_u,\, V_u\}$ is correspondingly determined by $a=a_n+\lambda$, $u(\theta)=\varepsilon\cos(n\theta)+\varepsilon v(\theta)$ with a zero point $(\lambda,\, v,\, \xi)$ of $H(\varepsilon;\, \lambda,\, v,\, \xi)=0$. Each step to obtain the solution for a given ε is composed of the following processes.

(I) Take an initial approximation γ_u which we except to be close to the required boundary.
(II) For a given γ_u, solve (1.1)′–(1.3)′.
(III) Modify the γ_u so that the conditions (1.4)–(1.5) are satisfied. From the fact described in § 1, this is equivalent to find a zero point of a mapping H.

Here we iterate (II) and (III) until the change of γ_u becomes smaller than a prescribed small value.

The most important character of the present paper is that we introduce the charge simulation method in solving the process (II). To explain this method, we choose N points y_j ($j=1, \cdots, N$) which are located outside γ_u as shown below. Let $y_j=(\rho_j, \phi_j)$ ($j=1, 2, \cdots, N$) be their

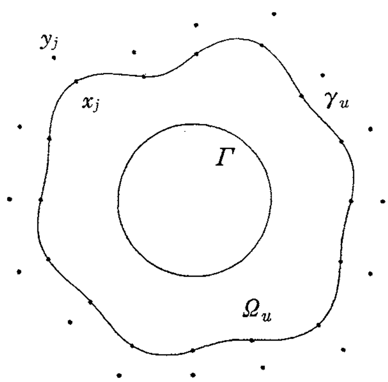

Figure 2

representations in the polar coordinates. For $x=(\zeta, \phi)\in\Omega_u$, let $G_k(\zeta, \phi)$ ($k=1, \cdots, N$) be the Green functions for $-\Delta$ in the outside of the unit circle with y_k as its singular point, respectively. It is given explicitly as

$$G_k(\zeta, \phi)=-\frac{1}{2\pi}\log\frac{|x-y_k|}{|y_k|\,|x-y_k^*|},$$

where y^* is the reflection of y with respect to Γ. Then we adopt $\tilde{V}_u$ of the following form as an approximate solution for V_u of (1.1)′–(1.3)′:

$$\tilde{V}_u(\zeta, \phi)=a\sum_{k=1}^{N}\alpha_k G_k(\zeta, \phi) \qquad (\alpha_k\in\boldsymbol{R},\ k=1, \cdots, N). \tag{2.1}$$

Such $\tilde{V}_u$ automatically satisfies the equation $\Delta\tilde{V}_u=0$ in Ω_u and the boundary condition $\tilde{V}_u|_{\Gamma}=0$ for any choice of $\{\alpha_k\}$. The boundary condition on γ_u determines $\{\alpha_k\}$. Namely, we choose N collocation points $x_j\equiv(\zeta_j, \phi_j)$, $j=1, 2, \cdots, N$, on γ_u (see Figure 2). Then $\{\alpha_k\}$ is determined so that $\tilde{V}_u$ satisfies $V_u|_{\gamma_u}=a$ at these N points x_j, i.e., $\{\alpha_k\}$ is the solution of

$$a\sum_k \alpha_k G_k(\zeta_j, \theta_j)=a \qquad (j=1, \cdots, N). \tag{2.2}$$

For such approximate function $\tilde{V}_u$, we consider the process (III). So we substitute $\tilde{V}_u$ for V_u appearing in the mapping H. Here we note that the equality $|\nabla\tilde{V}_u|^2=|(\partial/\partial r)\tilde{V}_u|^2+|(\partial/r\partial\theta)\tilde{V}_u|^2=|a\sum\alpha_k(\partial/\partial r)G_k|^2+|a\sum\alpha_k(\partial/r\partial\theta)G_k|^2$ holds true, where $(\partial/\partial r)G_k$ and $(\partial/\partial\theta)G_k$ are written concretely, and therefore, $|\nabla\tilde{V}_u|$ can be written concretely. In order to find a zero point of a discretized version of H, we prepare an approximate function space X_N. We divide the circle S^1 into N arcs of equal size, and put $\Delta\theta=\pi/N$ and $\theta_j=2(j-1)\cdot\Delta\theta$ for $j=1, 2, \cdots, N$. Let X_N be the set of all functions defined on S^1 which is constant on each of the subintervals $[\theta_j-\Delta\theta, \theta_j+\Delta\theta)$ $(j=1, 2, \cdots, N)$. The element v of X_N may be denoted by $\{v_1, v_2, \cdots, v_N\}$, where v_j is the value of v taken on $[\theta_j-\Delta\theta, \theta_j+\Delta\theta)$. We discretize the mapping by using the function space X_N for v.
And we take account of (2.2), where $x_j=(\zeta_j, \phi_j)$ $(j=1, 2, \cdots, N)$ are set as $\zeta_j=r_0+\varepsilon\cos(n\theta_j)+\varepsilon v_j$, $\phi_j=\theta_j$. Then we naturally get to the next nonlinear equations $H^N=0$ for the discretized version of $H=0$:

$$H^N=H^N(\varepsilon; \alpha, \lambda, v, \xi)=(H_0^N, H_1^N, H_2^N, H_3^N)$$
$$(\alpha=(\alpha_1, \alpha_2, \cdots, \alpha_N)\in\boldsymbol{R}^n, \quad v=(v_1, v_2, \cdots, v_N)\in X_N, \lambda, \xi\in\boldsymbol{R}),$$
$$(H_0^N)_j=\Big(\sum_{k=1}^N \alpha_k G_k(\zeta_j, \theta_j)-1\Big)(\lambda+a_n) \qquad (j=1, 2, \cdots, N),$$
$$(H_1^N)_j=\frac{1}{\varepsilon}\Big(\frac{1}{2}((\lambda+a_n)t_j)^2-\frac{g}{\zeta_j}+\sigma K_j-\xi_0-\xi\Big) \qquad (j=1, 2, \cdots, N),$$
$$(H_2^N)_1=\frac{1}{\varepsilon}\Big(\sum\frac{\pi}{N}\zeta_k^2-\pi-\omega_0\Big),$$
$$(H_3^N)_1=\sum v_k\frac{1}{n}(\sin(n(\theta_k+\Delta\theta))-\sin(n(\theta_k-\Delta\theta))),$$

where $\zeta_j=r_0+\varepsilon\cos(n\theta_j)+\varepsilon v_j$.

t_j and K_j are defined by

$$(\lambda+a_n)t_j=|\nabla\tilde{V}_u(r, \theta)|\,|_{(r,\theta)=(\gamma_j,\theta_j)},$$

$$K_j=\frac{\zeta_j^2+2\zeta_j'^2-\zeta_j\zeta_j''}{(\zeta_j^2+\zeta_j'^2)^{3/2}},$$

$$\zeta_j'=\frac{\zeta_{j+1}-\zeta_{j-1}}{4\cdot\Delta\theta},\qquad \zeta_j''=\frac{\zeta_{j+1}-2\zeta_j+\zeta_{j-1}}{4\cdot\Delta\theta^2}.$$

We note that $((\lambda+a_n)t_j)^2=|\nabla\tilde{V}_u(r,\theta)|^2|_{(r,\theta)=(r_j,\theta_j)}=|(\partial/\partial r)\tilde{V}_u|^2+|(\partial/r\partial\theta)\tilde{V}_u|^2=|(\lambda+a_n)\sum\alpha_k\cdot(\partial/\partial r)G_k|^2+|(\lambda+a_n)\sum\alpha_k\cdot(\partial/r\partial\theta)G_k|^2$ and $G_k(r,\theta)=-(1/4\pi)\times\log(r^2+\rho_k^2-2r\rho_k\cos(\theta-\theta_k))/(r^2\rho_k^2+1-2r\rho_k\cos(\theta-\theta_k))$, and hence, we can write t_j $(j=1,\cdots,N)$ concretely. The case of $\varepsilon=0$ is also written explicitly. In this way, we solve (II) and (III) at the same time.

Now that a zero point of H^N is an approximate solution of the bifurcating solution, we can find the approximate solution by the following Newton method: For a given ε, we start with initial values of $(\alpha^0, v^0, \lambda^0, \xi^0)$ which are suitably chosen, and solve

$$DH^N(\varepsilon;\alpha^m,v^m,\lambda^m,\xi^m)\cdot\begin{bmatrix}\alpha^{m+1}-\alpha^m\\ v^{m+1}-v^m\\ \lambda^{m+1}-\lambda^m\\ \xi^{m+1}-\xi^m\end{bmatrix}=-H^N(\varepsilon;\alpha^m,v^m,\lambda^m,\varepsilon^m),$$

where DH^N stands for the Jacobian matrix of H^N and its elements are described below.

We iterate this step until $|(\alpha^{m+1}, v^{m+1}, \lambda^{m+1}, \xi^{m+1})-(\alpha^m, v^m, \lambda^m, \xi^m)|$ becomes smaller than a prescribed small value. Then we adopt $(\alpha^{m+1}, v^{m+1}, \lambda^{m+1}, \xi^{m+1})$ as the solution for the given ε.

In the next step, we make ε a little larger. That is, we repeat the same procesure for $\varepsilon+\delta\varepsilon$ where $\delta\varepsilon$ is a small increment. We thus want to continue to get the other bifurcating solution from the same branch. In our computations, the solution for ε is used as the initial approximation in the next computation for $\varepsilon+\delta\varepsilon$.

We show DH^N concretely:

$$DH^N=\begin{bmatrix}\frac{\partial H_0^N}{\partial\alpha} & \frac{\partial H_0^N}{\partial v} & \frac{\partial H_0^N}{\partial\xi} & \frac{\partial H_0^N}{\partial\lambda}\\ \frac{\partial H_1^N}{\partial\alpha} & \frac{\partial H_1^N}{\partial v} & \frac{\partial H_1^N}{\partial\xi} & \frac{\partial H_1^N}{\partial\lambda}\\ \frac{\partial H_2^N}{\partial\alpha} & \frac{\partial H_2^N}{\partial v} & \frac{\partial H_2^N}{\partial\xi} & \frac{\partial H_2^N}{\partial\lambda}\\ \frac{\partial H_3^N}{\partial\alpha} & \frac{\partial H_3^N}{\partial v} & \frac{\partial H_3^N}{\partial\xi} & \frac{\partial H_3^N}{\partial\lambda}\end{bmatrix}$$

$$
=\left[\begin{array}{c:c:c:c}
\boldsymbol{C}_{11} & \boldsymbol{C}_{12} & \begin{matrix}0\\ \vdots\\ 0\end{matrix} & \boldsymbol{C}_{14} \\
\hdashline
\boldsymbol{C}_{21} & \boldsymbol{C}_{22} & \begin{matrix}-1\\ \vdots\\ -1\end{matrix} & \boldsymbol{C}_{24} \\
\hdashline
0\cdots 0 & \boldsymbol{C}_{32} & 0 & 0 \\
\hdashline
0\cdots 0 & \boldsymbol{C}_{42} & 0 & 0
\end{array}\right],
$$

$(\boldsymbol{C}_{11})_{jk}=a\cdot G_k(\gamma_j,\ \theta_j)\cdot\delta_{jk}$ where $a=\lambda+a_n$, δ_{jk} is Cronecker's delta,

$$(\boldsymbol{C}_{12})_{jk}=a\cdot\sum_k \alpha_k\frac{\partial}{\partial v_k}G_k(\gamma_j,\ \theta_j)\cdot\delta_{jk},$$

$$(\boldsymbol{C}_{14})_j=\sum_k \alpha_k G_k(\gamma_j,\ \theta_j)-1,$$

$$(\boldsymbol{C}_{21})_{jk}=\frac{1}{\varepsilon}a^2 t_j\frac{\partial}{\partial n}G_k(\gamma_j,\ \theta_j),$$

$$
\begin{aligned}
(\boldsymbol{C}_{22})_{jk}=\frac{1}{\varepsilon}\Bigg(a^2 t_j\Bigg\{&\sum_i \alpha_i\frac{\partial^2}{\partial v_k\partial n}G_i(\gamma_j,\ \theta_j)\cdot\delta_{jk}\\
&+\sum_i \alpha_i\frac{\partial^2}{\partial v_k'\partial n}G_i(\gamma_j,\ \theta_j)\cdot\frac{\delta_{j,k+1}-\delta_{j,k-1}}{4\cdot\Delta\theta}\Bigg\}\\
&+\sigma\left\{\frac{\partial K_j}{\partial v_k}\cdot\delta_{jk}+\frac{\partial K_j}{\partial v_k'}\cdot\frac{\delta_{j,k+1}-\delta_{j,k-1}}{4\cdot\Delta\theta}+\frac{\partial K_j}{\partial v_k''}\cdot\frac{\delta_{j,k+1}-2\delta_{j,k}+\delta_{j,k-1}}{4\cdot\Delta\theta^2}\right\}\Bigg),
\end{aligned}
$$

$$(\boldsymbol{C}_{24})_j=\frac{2}{\varepsilon}a t_j^2,$$

$$(\boldsymbol{C}_{32}^T)_j=\frac{2\pi}{N}\gamma_j,$$

$$(\boldsymbol{C}_{42}^T)_j=\frac{1}{n}(\sin(n(\theta+\Delta\theta))-\sin(n(\theta-\Delta\theta))).$$

This gives a complete description of our iteration scheme.

§3. Experimental results.

We show our results in Figures 3–5. Similarly to our previous work [2], we again restricted ourselves to branches only from a_1 and from a_2, and we put $r_0=2$ and $g=1$. In [2] the computations are restricted to a rather small region of a and σ. According to the present method (the charge simulation method), we can perform computations for a wider region of $(a,\ \sigma)$, especially for small a and σ. The solutions which were obtained in [2] are also computed by the present scheme anew. Then we notice that they are the same. In Figures 3-5 we present solutions which are obtained newly by the present scheme.

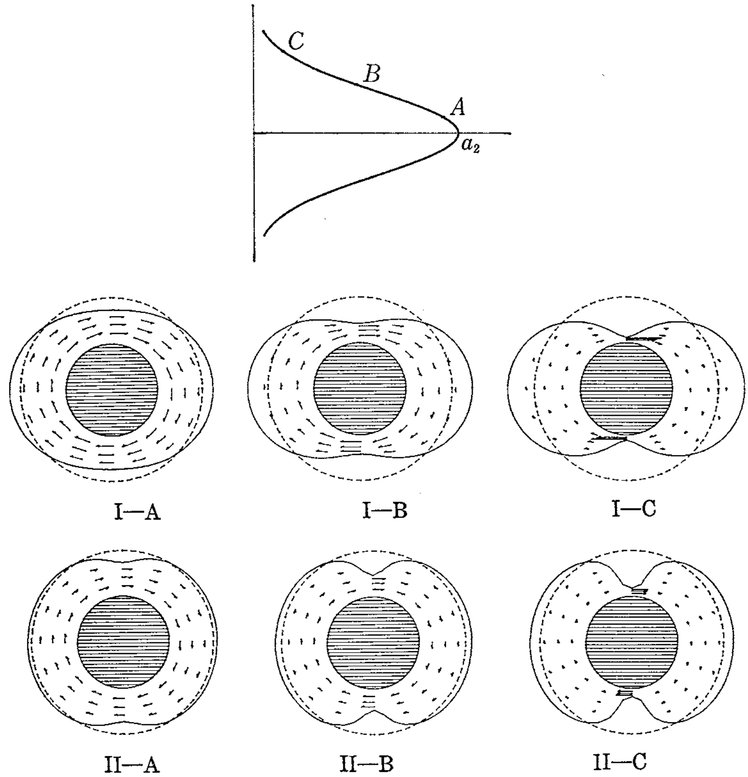

Figure 3 I: $\sigma=5$
II: $\sigma=0.07$

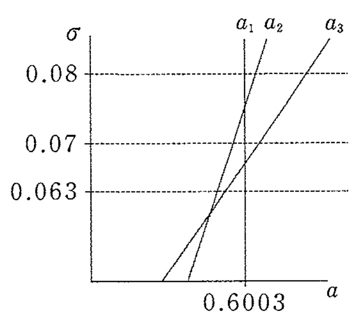

Figure 4

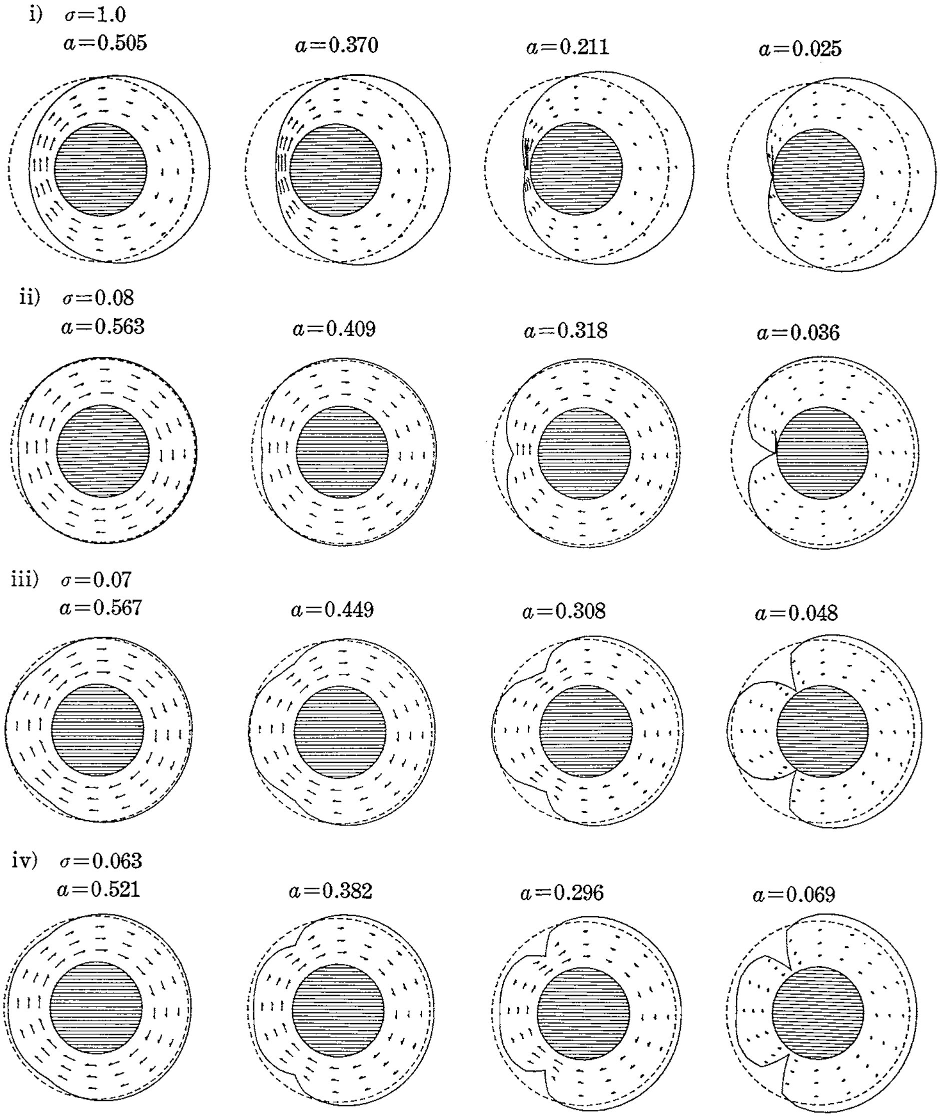

Figure 5

Figure 3 shows the a_2-branch, Figure 4 is for the relation of σ to a_1, a_2 and a_3, and Figure 5 shows the bifurcating solutions of the a_1-branch when σ takes various values. The arrows in these figures indicate velosity vectors, and their length is proportional to flow speed. As one can see from Figure 4, there are intersections of bifurcation sets for small σ. This occurs only when the surface tension is small. The method in [2] does not work in the case where σ is so small that the intersection takes place. Here is our advantage to employ the charge simulation method, by which we can analyze the case of small σ. When σ is very close to the value at which the intersection in Figure 4 occurs, the secondary bifurcations do take place.

The number of dents in the shape of bifurcating solutions changes from one to two or three, according as the order of a_1, a_2, a_3 changes depending on the value σ. We believe that this is a consequence of the existence of secondary bifurcations. Our purpose is to realize the global bifurcation diagram by simulation. Or we want to see the mechanism of secondary bifurcations, because only their existence is known analytically. But, in order to do this, however, a highly accurate simulation is required. Actually, when σ is 0.07, a_1 is 0.6003 and a_2 is 0.5966, the difficulty in implementing our calculation was considerable since non-trivial solutions exist extremely densely around there.

In the next section, we will mention accuracy of our numerical treatments and error estimation about the charge simulation method.

§4. Examination and conclusion.

In this section we examine the precision of the charge simulation method (hereafter we write this as the CSM). At first, for simplicity, we consider a Dirichlet problem in the fixed domain with $\gamma=\gamma_0$. Let Γ, γ_0 and Ω_{γ_0} be as before, and let V be a solution of $\Delta V=0$ in Ω_γ, $V|_\Gamma=0$ and $V|_{\gamma_0}=1$. The discretization is made in the same way with §2. And we adopt the following $\tilde{V}$ as an approximate function for V:

$$\tilde{V}(r,\theta)=\sum_{j=1}^{N}\alpha_j\cdot G_j(r,\theta) \qquad \text{for} \quad x=(r,\theta)\in\Omega_\gamma,$$

$$\text{where } G_j(r,\theta)=-\frac{1}{4\pi}\log\frac{r^2+\rho^2-2r\rho\cos(\theta-\theta_j)}{r^2\rho^2+1-2r\rho\cos(\theta-\theta_j)},$$

$$\theta_j=(2j-2)\cdot\Delta\theta, \quad \Delta\theta=\frac{\pi}{N}, \quad \theta_{N+1}=\theta_1, \quad \rho>r_0.$$

The boundary condition $\tilde{V}|_{\gamma_0}=1$ implies the following linear equations.

$$M\cdot\alpha=I, \tag{4.1}$$

where

$$M=\begin{bmatrix} g_1 & g_2 & \cdots & g_N \\ g_N & g_1 & \cdots & g_{N-1} \\ \vdots & \vdots & & \vdots \\ g_2 & g_3 & \cdots & g_1 \end{bmatrix}, \quad \alpha=\begin{bmatrix} \alpha_1 \\ \alpha_2 \\ \vdots \\ \alpha_N \end{bmatrix}, \quad I=\begin{bmatrix} 1 \\ 1 \\ \vdots \\ 1 \end{bmatrix},$$

$$g_j=G_j(r_0, \theta)=-\frac{1}{4\pi}\log\frac{r_0^2+\rho^2-2r_0\rho\cos\theta_j}{r_0^2\rho^2+1-2r_0\rho\cos\theta_j}.$$

This matrix M is cyclic, so α can be given exactly as

$$\alpha_1=\alpha_2=\cdots=\alpha_N=\frac{1}{\sum g_j},$$

and $\tilde{V}$ is given by

$$\tilde{V}(r, \theta)=\frac{\sum G_j(r, \theta)}{\sum g_j}.$$

Now we put an error function $e(r, \theta)$ as

$$e(r, \theta)=\tilde{V}(r, \theta)-V(r, \theta).$$

Because $\tilde{V}$ and V are harmonic in Ω_γ, $e(r, \theta)$ is also harmonic in Ω_γ. Therefore $|e(r, \theta)|$ has its maximum value on the boundary, and $e(r, \theta)|_\Gamma=0$ is satisfied automatically. So we may estimate $e(r, \theta)$ only on the boundary $\gamma_0: e(r, \theta)|_{\gamma_0}=e(r_0, \theta)=\sum G_j(r_0, \theta)/\sum g_j-1$.
We can see that $e(r_0, \theta)$ vanishes at $\theta=\theta_j$ $(j=1, 2, \cdots, N)$ and has its extremum at $\theta=(\theta_j+\theta_{j+1})/2$ $(j=1, 2, \cdots, N)$ because it is symmetric. We put the extremum as $e_h(\rho)$, then it is writen as

$$e_h(\rho)=\frac{\sum\log\dfrac{r_0^2+\rho^2-2r_0\rho\cos(\theta_j+\Delta\theta)}{r_0^2\rho^2+1-2r_0\rho\cos(\theta_j+\Delta\theta)}}{\sum\log\dfrac{r_0^2+\rho^2-2r_0\rho\cos(\theta_j)}{r_0^2\rho^2+1-2r_0\rho\cos(\theta_j)}}-1.$$

We regard $e_h(\rho)$ as a function of h $(=2r_0\cdot\Delta\theta)$ and ρ, and examine the asymptotic behavior by plotting its graph (see Figure 6). Then we see $e_h(\rho)\to 0$ as $\rho\to\infty$ if h is fixed, and $e_h(\rho)\to 0$ as $h\to 0$ (i.e. $N\to\infty$) if ρ is fixed.
In fact,

$$e_h(\rho)\xrightarrow[h\to 0]{}\frac{\displaystyle\int_0^{2\pi}\log\frac{r_0^2+\rho^2-2r_0\rho\cos\theta}{r_0^2\rho^2+1-2r_0\rho\cos\theta}d\theta}{\displaystyle\int_0^{2\pi}\log\frac{r_0^2+\rho^2-2r_0\rho\cos\theta}{r_0^2\rho^2+1-2r_0\rho\cos\theta}d\theta}-1=0 \qquad \text{for every } \rho,$$

and

$$e_h(\rho)=\frac{\sum \log \dfrac{\left(\dfrac{r_0}{\rho}\right)^2+1-2\left(\dfrac{r_0}{\rho}\right)\cos(\theta_j+\Delta\theta)}{r_0^2+\left(\dfrac{1}{\rho}\right)^2-2\left(\dfrac{r_0}{\rho}\right)\cos(\theta_j+\Delta\theta)}}{\sum \log \dfrac{\left(\dfrac{r_0}{\rho}\right)^2+1-2\left(\dfrac{r_0}{\rho}\right)\cos(\theta_j)}{r_0^2+\left(\dfrac{1}{\rho}\right)^2-2\left(\dfrac{r_0}{\rho}\right)\cos(\theta_j)}}-1$$

$$\xrightarrow[\rho\to\infty]{} \frac{\sum \log\left(\dfrac{1}{r_0}\right)^2}{\sum \log\left(\dfrac{1}{r_0}\right)^2}-1=0 \qquad \text{for any } h.$$

From Figure 6, we may roughly regard as $-\log|e_h(\rho)|=O(h^{-1}\cdot(\rho/r_0))$.

On the other hand, we check on the condition number of matrix M. Generally in $M\cdot\alpha=\beta$, let α be $\alpha+\Delta\alpha$ if $M\to M+\Delta M$ and $\beta\to\beta+\Delta\beta$, then we get the following relation.

$$(4.2) \qquad \frac{\|\Delta\alpha\|}{\|\alpha\|}\leqq\frac{\mu}{1-\mu\dfrac{\|\Delta M\|}{\|M\|}}\left(\frac{\|\Delta M\|}{\|M\|}+\frac{\|\Delta\beta\|}{\|\beta\|}\right),$$

where $\mu=\|M\|\cdot\|M^{-1}\|$ is what is called the condition number of M. Because M is symmetric and cyclic, its eigenvalues λ_k $(k=1, 2, \cdots, N)$ and its condition number μ are given as

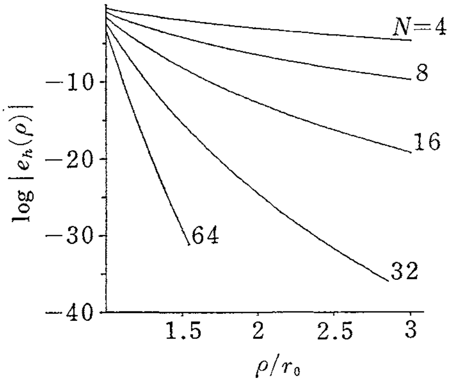

Figure 6

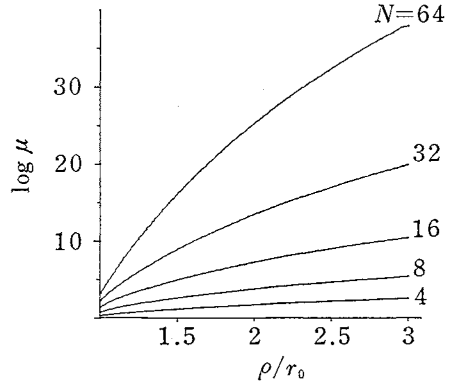

Figure 7

$$\lambda_k = \sum_{j=1}^{N} g_j \cdot \omega_k^{j-1} = \sum_{j=1}^{N} g_j \cdot \cos(2(j-1)(k-1)\Delta\theta) \qquad (k=1, \cdots, N),$$

where $\omega_k = e^{i\cdot 2(k-1)\cdot\Delta\theta}$, $i=\sqrt{-1}$,

$$\mu = \frac{\max \lambda_k}{\min \lambda_k} = \frac{\lambda_1}{\lambda_{N/2+1}} \qquad \text{(if } N \text{ is even)}.$$

Similarly to $e_h(\rho)$, regarding μ as a function of h and ρ, we examine the asymptotic behavior by plotting its graph (see Figure 7). Then contrary to $e_h(\rho)$, we may roughly regard as $-\log \mu = O(h\cdot(\rho/r_0)^{-1})$. Namely the better the approximation of the series is, the worse the matrix condition is.

Next we consider the case where γ is a circle γ_β which is slightly translated from γ_0, i.e., $\gamma_\beta = \{(u, v) \mid (u-\beta)^2+v^2=r_0^2,\ 0<\beta<r_0-1\}$ and $\Omega_\beta = \{(u, v) \mid 1<u^2+v^2,\ (u-\beta)^2+v^2<r_0^2\}$. We note that Ω_β in z-plane is mapped over $D_\beta = \{(\xi, \nu) \mid (1+\beta p)^2<\xi^2+\nu^2<r_0^2\}$ in ζ-plane by the following conformal mapping:

$$\zeta = (1+\beta p)\frac{z+p}{pz+1}, \qquad \text{where } z=u+iv,\ \zeta=\xi+i\nu,\ i=\sqrt{-1},$$

$$= f(z), \qquad p = \frac{2\beta}{r_0^2-1-\beta^2+((r_0^2-1-\beta^2)^2-4\beta^2)^{-1/2}}.$$

By this mapping, Γ and γ_β are mapped over two concentric circles $\{|\zeta|=1+\beta p\}$ and $\{|\zeta|=r_0\}$ respectively, and D_β is an annular domain similarly to Ω_γ. Considering in ζ-plane, we see that it is the best to take collocation and singular points as before. Namely we put them on the points which are located with equal distance in concentric circle. Therefore we can get their optimal positions in z-plane by the inverse mapping from ζ-plane. We show the example for the case of $\beta=0.5$ in Figure 8.

As mentioned above, the precision of the CSM depends on the way to take the collocation and singular points. In the case that Ω_γ is an annular domain or is a region conformally equivalent to an annular domain, we can easily find their optimal positions. And the approximation error can be reduced exponentially with respect to $h\cdot(\rho/r_0)^{-1}$, while the condition number is within the machine epsilon. In other cases, we must rely on numerical experiments. Indeed, the effective methods to find the optimal positions of collocation and singular points

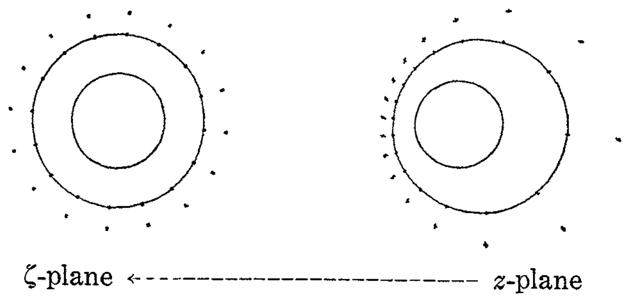

$$\zeta = f(z) = (1+\beta p)\frac{z+p}{pz+1}$$

$$\tilde{G}_k = -\frac{1}{4\pi}\log\frac{(1+\beta p)|\chi - \upsilon_k|}{|\upsilon_k|\,|\chi-\upsilon_k^*|} \quad \text{where } \upsilon_k\cdot\upsilon_k^* = (1+\beta p)^2 \text{ in } \zeta\text{-plane},$$

$$G_k = -\frac{1}{4\pi}\log\frac{(1+\beta p)|f(x)-f(y_k)|}{|f(y_k)|\,|f(x)-f(y_k^*)|} = -\frac{1}{4\pi}\log\frac{|x-y_k|}{|y_k|\,|x-y_k^*|} \quad \text{in } z\text{-plane}.$$

Figure 8

in general domain have not been found yet. Practically, they are chosen by trial and error based on expriments for each problem. According to the results established so far,[3] we know that it is better to take collocation points more densely in a neighborhood where the curvature is larger or the depth is smaller, and to take the singular points in such a way that $h_j\cdot(\rho_j/r_j)^{-1}=f_j$ $(j=1, 2, \cdots, N)$ are almost constant.

In view of these facts, we carried out our computations. However in our case, we use iterative computations by the Newton method. So we must take into account the following. That is, in (4.2), both of $\|\varDelta M\|$ and $\|\varDelta\beta\|$ have values not so small in the case of iterative computation. Therefore it needs to restrict μ so small that $\|\varDelta\alpha\|$ is not so large to exceed a convergence region of the Newton method. Namely, in this case, f_j cannot be taken so small as in the case of a fixed domain. Here $\|\varDelta M\|$ and $\|\varDelta\beta\|$ are influenced by the value of increment $\delta\varepsilon$ appearing in step. 2 of §2. In fact, if $\delta\varepsilon$ is taken smaller, then $\|\varDelta M\|$ and $\|\varDelta\beta\|$ are smaller. In consideration of these conditions for the case of $N=32$, $r_0=2$ and $\delta\varepsilon=0.1$, it turns out to be optimal to take ρ about from 2.5 to 2.8, and then the absolute error is about 10^{-5}. In our experimental results, the errors were bounded in about $10^{-4}\sim10^{-3}$ in the neighborhood of the trivial solution for the above case, if σ is not so small. When σ is smaller, nonlinearity is stronger and we must take $\delta\varepsilon$ smaller. Where the boundary γ is far from the trivial position or is tortuous, it is very difficult to find optimal condition. Moreover, whether it converges or not is sensitively affected by the way to take values of $\{f_j\}$. In our computations, collocation and singular points are determined in the following way. The θ-coordinates of collocation points are fixed. We estimated the mean square of errors on examination points at every step, and if necessary, we changed only the distances of the singular points from the origin and computed over again. Here the examination points are taken between collocation points. The results shown here are the case of which the collocation points are $x_j=(\zeta_j, \theta_j)=(\zeta_j, 2(j-1)\pi/N)$ and the singular points are $y_j=(\rho_j, \theta_j)$, where ρ_j are taken so that $\rho_j/\gamma_j=f_j=$constant. We examined by replacing both of these sets of points variously, but we were not able to find remarkable improvements. However, we expect to improve these results including the error bounds in some way or other. Though analysis of the CSM has many points to explore, we think that our results are reliable to a certain extent because we can estimate the approximation error numerically in the way above.

Finally, we make some comparisons of these results with those by the BEM (Boundary Element Method).

(1) The number of iterations in the Newton method is about 4 or 5 in the BEM (the epsilon of convergence ε was taken as 10^{-4}), and is about 3 to 4 in the CSM ($\varepsilon=10^{-5}$).

(2) As for the CPU time in the region of ill conditions, it takes for the BEM about 10~20 times more than the CSM. The reason of this is as follows. In the BEM, more than 80% of its CPU time is exhausted in numerical integrations because of using linear elements.

(3) The accuracy of the CSM is better than that of the BEM. Because, by the BEM we could not simulate in the range where the surface tension σ is small or the nonlinearity is remarkable. We think that this is firstly because the numerical integration of singular functions in the BEM is less accurate and secondary because we use a Quasi-Newton method in the BEM, while a Newton method is used in the CSM. We note that, for instance in the scheme in [2], the exact Newton method cannot be used.

(4) In the CSM, it is useful that the derivative of solution is calculated as a linear sum of derivatives of Green's function. So we can easily obtain the velocity vector inside the flow region.

In general, we might conclude that the charge simulation method is powerful method to solve potential problems. We hope to analyze it mathematically elsewhere.

References

[1] Crandall, M. G. and P. M. Rabinowitz, Bifurcation from simple eigenvalue, J. Funct. Anal. **8** (1971), 321–340.

[2] Fujita, H., Okamoto, H. and M. Shōji, A numerical approach to a free boundary problem for a perfect fluid with surface tension, Japan J. Appl. Math. **2** (1985), 197–210.

[3] Murashima, S., Daiyou Denkahou to sono Ouyou, (in Japanese) Morikita Syuppan, Tokyo, 1983.

[4] Okamoto, H., Stationary free boundary problems for circular flows with or without surface tension, Proc. of U.S.-Japan Seminar on Nonlinear P.D.E. in Applied Sci. (ed. H. Fujita, P.D. Lax and G. Strang), Lecture Notes Numer. Appl. Anal. No. 5, Kinokuniya Book Store, Tokyo, 1982, 233–251.

[5] Okamoto, H., Bifurcation phenomena in a free boundary problem for a circulating flow with surface tension, Math. Methods Appl. Sci. **6** (1984), 215–233.

[6] Okamoto, H., Nonstationary or Stationary Free Boundary Problems for Perfect Fluid with Surface Tension, Lecture Notes in Numer. Appl. Anal. No. 6, Kinokuniya Book Store, Tokyo, 1983, 143–154.

[7] Okamoto, H. and M. Shōji, Dynamical system arising in nonstationary motion of a free boundary of a perfect fluid, Sûrikaisekikenkyûsho Kôkyûroku **559** (1985), 19–41.

(Received November 21, 1985)

Department of Mathematics
Faculty of Science
University of Tokyo
Hongo, Tokyo
113 Japan